

Thermo-mechanical behaviour of floating energy pile groups in sand*

Huai-feng PENG¹, Gang-qiang KONG^{†‡1}, Han-long LIU^{1,2}, Hossam ABUEL-NAGA³, Yao-hu HAO¹

¹Key Laboratory of Geomechanics and Embankment Dam Engineering, Hohai University, Nanjing 210098, China

²Key Laboratory of New Technology for Construction of Cities in Mountain Area, Chongqing University, Chongqing 400045, China

³College of Science, Health and Engineering, La Trobe University, Victoria 3086, Australia

[†]E-mail: gqkong1@163.com

Received Aug. 29, 2017; Revision accepted Jan. 10, 2018; Crosschecked July 9, 2018

Abstract: This paper presents the experimental results of small-scale model tests of an instrumented floating energy pile group in which the piles were embedded in dry medium-dense sand and subjected to the seasonal temperature pattern of the city of Nanjing in China. The study also included a model test to assess the effect of including nonthermal piles on the thermo-mechanical behaviour of the floating energy pile group. For comparison, a model test of a single floating energy pile embedded in the same soil and subjected to a similar temperature pattern was also conducted. The results show that the thermo-mechanical behaviour of an energy pile group is different from that of a single energy pile in terms of the thermally induced change in axial pile stress and the displacement of the pile top and tip. This difference in behaviour could be explained by the higher lateral confining pressure expected on a single pile than on a pile in a group due to pile interaction effects, which could lead to different end restraint boundary conditions. We conclude that the thermo-mechanical behaviour of an energy pile is controlled mainly by the end restraint boundary conditions.

Key words: Energy pile; Floating pile; Pile group; Nonuniform thermal; Nonuniform displacement
<https://doi.org/10.1631/jzus.A1700460>

CLC number: TU473.1

1 Introduction

Energy piles are one of the energy geostructures most widely used around the world. They act not only as load-bearing elements, but also as an alternative thermal energy source. However, changing the temperature of the pile and surrounding soil may induce irreversible strains, leading to stress redistribution and nonuniform displacement in the energy pile. These thermal effects are more obvious in the energy

pile group compared to the single energy pile, especially in the case of nonuniform heating of an energy pile group in which some of the piles are not thermally active (nonthermal piles). As a result, the serviceability and safety of energy pile-supported structures may be affected (Di Donna and Laloui, 2015; Wang TF et al., 2016).

Several studies have been directed to understand the thermo-mechanical behaviour of a single energy pile using small-scale model tests, centrifuge model tests, and full-scale tests (Laloui et al., 2006; Bourne-Webb et al., 2009; McCartney and Rosenberg, 2011; Kalantidou et al., 2012; Ng et al., 2014; Stewart and McCartney, 2014; Wang B et al., 2014; Goode III and McCartney, 2015; Liu et al., 2016; Wang CL et al., 2016, 2017). The results of these studies indicated that the end restraint of the energy pile and the geotechnical properties of the surrounding soil control

[‡] Corresponding author

* Project supported by the National Natural Science Foundation of China (No. 51778212) and the Fundamental Research Funds for the Central Universities (Nos. KYLX16_0725 and 2016B42914), China

 ORCID: Huai-feng PENG, <https://orcid.org/0000-0002-9357-4307>; Gang-qiang KONG, <https://orcid.org/0000-0002-0645-5140>

© Zhejiang University and Springer-Verlag GmbH Germany, part of Springer Nature 2018

the engineering behaviour of the energy pile. However, as piles are almost always installed in groups, the temperature effects on the design of a pile group should also be investigated. Table 1 lists most of the published field tests and numerical studies that have investigated the thermo-mechanical behaviour of energy pile groups.

Jeong et al. (2014) conducted a numerical investigation to determine the influence of pile spacing and arrangement, soil type, and end bearing condition on the thermo-mechanical behaviour of an energy pile group. The results highlighted the effect of the pile cap on the thermally induced axial pile load. Salciarini et al. (2013) conducted numerical simulations to assess the thermo-mechanical behaviour of an energy pile group where some of the energy piles in the group were nonthermal piles. Their results revealed that the maximum thermally induced pile load redistribution occurs at the very early stage of the thermal exchange process, as at this stage the differences in temperature between thermal and nonthermal piles were the largest.

Saggu and Chakraborty (2016) also used a numerical approach to investigate the thermo-mechanical response of energy pile groups in sand

where different combinations of thermal and non-thermal piles in the group were simulated. Their simulations showed that for the groups that contained both thermal and nonthermal piles, differential settlement at the pile base is expected. Rotta Loria and Laloui (2017a) conducted an extensive numerical experimental program to estimate the vertical displacement of energy pile groups subjected to thermal loads and proposed a simplified interaction factor method for energy pile groups. Further work in this regard was recently presented by Rotta Loria and Laloui (2017b, 2017c). The results of the field experimental study by Mimouni and Laloui (2015) highlighted the importance of considering the different thermal operation conditions (thermal or non-thermal) of energy piles in a group, as different thermal conditions could lead to different thermo-mechanical responses.

Based on the above discussion and the results of the previous studies (Table 1), it is clear that more experimental studies are required to understand the thermo-mechanical behaviour of energy pile groups. To our knowledge, the thermo-mechanical behaviour of floating energy pile groups embedded in dry sand

Table 1 Summary details of some energy group pile tests using experimental and numerical approaches

Study	Test method	Pile length (cm)	Pile diameter (cm)	Soil on shaft	Pile type	Arrangement of piles
Mimouni and Laloui (2015), Rotta Loria and Laloui (2017a)	Experimental, numerical	2500	96–117	Soft clay/ Stiff till	Semi-floating pile	
Murphy et al. (2015)	Experimental	1520	61	Sand and gravel	End bearing pile	
You et al. (2014, 2016)	Experimental	1800	42	Sandy silt/ Clay/Gravel	Semi-floating pile	
Salciarini et al. (2013)	Numerical	2500	100	Dense sand/ Clay/Gravel	Semi-floating pile	
Salciarini et al. (2017)	Numerical	2500	60	Stiff clay	Semi-floating pile	
Saggu and Chakraborty (2016)	Numerical	2000	100	Sand	Semi-floating pile	
Jeong et al. (2014)	Numerical	2000	50	Sand/Clay	Semi-floating pile	
This study	Experimental	150	9	Sand	Floating pile	

● is the energy pile; ○ is the normal pile; ■ is the anchor pile

has not yet been investigated. The main aim of this study is to assess the thermo-mechanical behaviour of this type of energy pile group.

2 Test setup and materials

Fig. 1 shows a schematic plan and elevation views of the test model tank (width: 2 m; length: 3 m; depth: 1.7 m) which included a total of 11 precast concrete piles that were installed in a sand bed. The energy pile had a diameter (D) of 90 mm and length of 1500 mm (Fig. 2). Each model energy pile comprised a U-shaped polyvinyl chloride (PVC) circulation tube with an outer diameter of 10 mm and an inner diameter of 8 mm. The surface of the model energy pile was coated with sand that was mixed with cement to mimic the roughness of a full-scale pile surface. The thermal properties of the model energy pile and

the geotechnical properties of the Nanjing river sand that was used in this study are listed in Table 2 and Fig. 3.

Nine of the piles formed a square pattern pile group in which the pile spacing was $3D$ center to center. The remaining two piles were used to test single pile behaviour and were placed separately at a distance of 890 mm from the edge of the pile group. The distance between the two single piles was $6D$. To guarantee the floating condition for the piles, a spring of known stiffness (76 N/mm), a protective sleeve, and a load cell were attached to the base of the piles (Figs. 1 and 2). The load cell and the spring were used to measure the pile base displacement. After setting up the floating piles in the empty model tank and holding them in place, a pluviation approach (sand raining technique) was used to fill the model tank with a uniform sand layer at a relative density of 70% (Lo Presti et al., 1993; Dave and Dasaka, 2012;

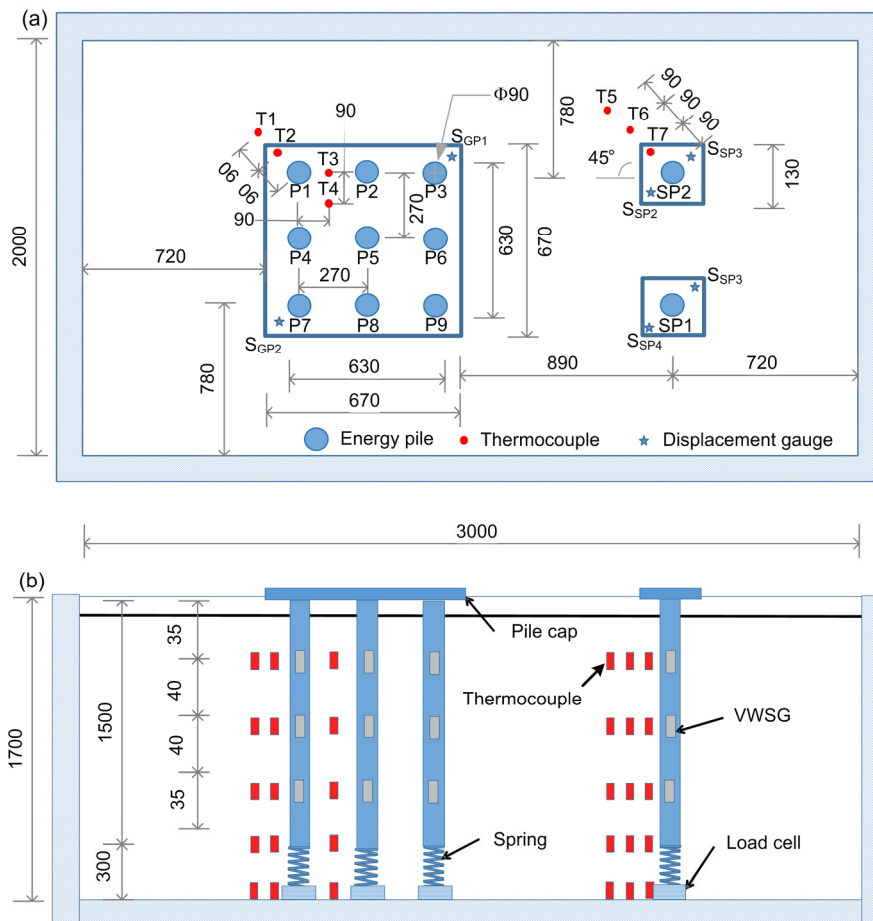


Fig. 1 Layout of model test and the energy piles with sensors: (a) cross section; (b) vertical section (unit: mm)
VWSG indicates vibrating wire strain gauge

Hariprasad et al., 2016). At the end of this process a steel pile cap of 10 mm thickness was fixed to the pile group at a distance of 100 mm above the top surface of the sand layer (free-standing condition; Fig. 1).

To monitor the axial pile strain, the model energy pile was equipped with three vibrating wire strain gauges (VWSGs) installed at different locations throughout the length of the pile (Fig. 2). The load cell and the spring at the tip of the pile were used to

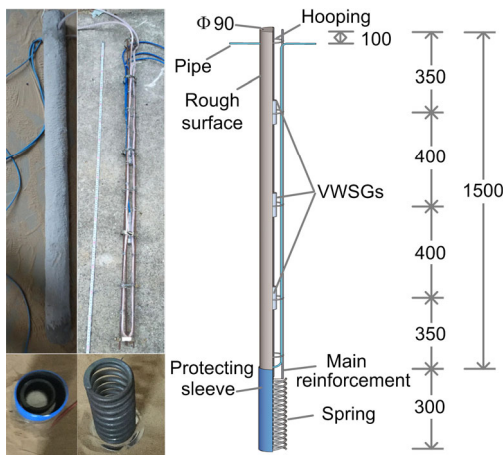


Fig. 2 Layout of model pile with sensors installed on the reinforcing cage (unit: mm)

Table 2 Mechanical and thermal properties of sand and concrete used in this study

Parameter	Value
Sand	
Mean particle size, D_{50} (mm)	0.32
Coefficient of uniformity, C_u	2.5
Coefficient of curvature, C_c	1.49
Specific gravity, G_s	2.71
Maximum dry density, $\rho_{d,max}$ (g/cm^3)	1.695
Minimum dry density, $\rho_{d,min}$ (g/cm^3)	1.34
Nature dry density, ρ_d (g/cm^3)	1.55
Critical state friction angle, ϕ_c ($^\circ$)	31
Thermal conductivity, λ (W/(m·K))	0.276
Special heat capacity, C (J/(kg· $^\circ$ C))	876
Thermal diffusivity, α (mm^2/s)	0.197
Concrete	
Elasticity modulus, E (MPa)	3.03×10^4
Poisson's ratio, ν	0.2
Thermal conductivity, λ (W/(m·K))	1.4
Special heat capacity, C (J/(kg· $^\circ$ C))	880
Thermal diffusivity, α (mm^2/s)	0.663

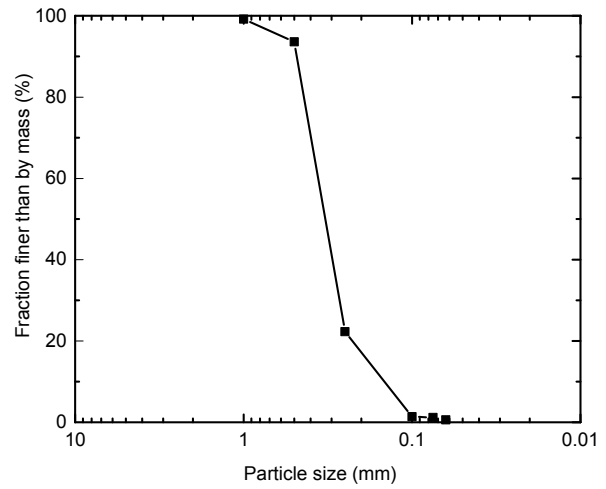


Fig. 3 Particle size distribution of sand used in model test

monitor the pile tip displacement and a set of displacement transducers (linear variable differential transformer) were used to measure the pile cap displacement (Fig. 1). Several thermocouples were installed at different locations in the model tank to measure the change in sand temperature due to heat exchange with the energy pile.

3 Scale and boundary effects

The model test described in this paper was designed carefully to minimize both mechanical and thermal boundary effects and the possible scale effect caused by the ratio of mean particle size D_{50} to the pile diameter D . According to Kraft Jr (1991) and Salgado et al. (1998) for axial pile load tests on non-displacement piles in sand, the radius of the influence zone around the pile is about $4D$ to $5D$. In this study, the distance from the edge of energy pile group to the model tank wall was $5.5D$. Furthermore, as the ratio between the pile diameter D and mean particle size D_{50} was very small in this study (0.003), shear stress mobilization along the pile shaft was not expected. Thermal boundary effects were also considered by adding a thermal insulation layer to the wall of the model tank and installing the model tank below the ground surface to reduce the effect of ambient temperature fluctuations on the test results.

As the energy pile group in this study was subjected to the seasonal temperature pattern of the city of Nanjing in China, this temperature pattern needed

to be scaled down to suit the geometrical configuration of the model tank. Li and Lai (2015) showed that the Fourier number Fo is a reasonable approach to compare the time scales of a laboratory scale model test and a full-scale model test where the Fourier number Fo is expressed as

$$Fo = \frac{\alpha_s t}{r_p^2}, \quad (1)$$

where t is the time, r_p is the pile radius, and α_s is the thermal diffusivity of the soil. Based on the Fo concept, the seasonal temperature pattern of the city of Nanjing, and the geometrical configuration of the model tank, the inlet temperature pattern of the energy piles in this study over a year is depicted in Fig. 4. Fig. 5 shows a comparison between the temperature patterns used in the previous study based on a Fourier number approach.

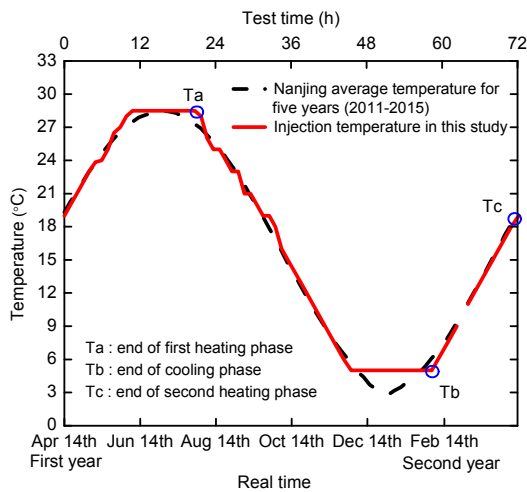


Fig. 4 Injection temperature selection used in this study

4 Experimental programs

The experimental program in this study comprised single pile (SP) and group pile testing programs (Table 3). In the single pile testing program two model tests (Test 1, Test 2) were conducted. The pile in Test 1 was loaded incrementally to determine the ultimate pile load capacity at room temperature (19 °C) (Fig. 6). The pile in Test 2 was subjected to 1.23 kN (50% of the pile load capacity) then the

water circulation process through the pile started in which the inlet water temperature followed the temperature pattern shown in Fig. 5. Changes in the temperature of the surrounding soil and the thermally induced pile displacement and axial forces were monitored to assess the thermo-mechanical behaviour of the single floating energy pile in sand.

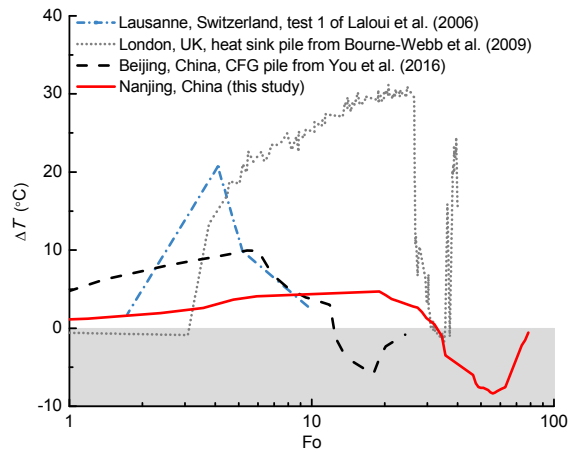


Fig. 5 Temperature changes of piles during tests

The pile group testing program comprised three tests (Table 3). Test 3 was designed to determine the ultimate pile group capacity at room temperature (19 °C) (Fig. 6). To provide a good comparison of the load-settlement curves from the individual and group piles, a curve was included with a load of $9Q$ (Q is load applied to the SP1) and settlement the same as SP1 in Fig. 6. The results show that the ultimate load of the pile group was only 76% of that of the single pile carrying the same total load. For Test 3, the loads of the pile tips recorded by the base load cells at different loading steps were very small (Fig. 7). This result confirmed that the piles installed in the model tank could be classified as floating piles. In Test 4, after loading the energy pile group up to 11 kN, the heat exchange circulation process through nine piles in the group started in which the inlet water temperature followed the temperature pattern shown in Fig. 5. To assess the thermo-mechanical behaviour of the floating energy pile group in sand, the surrounding soil temperature changes and the thermally induced pile displacement and axial forces were monitored. Test 5 was similar to Test 4 except that some of the piles in Test 5 were not thermally active (nonthermal).

The results of Test 5 were expected to enhance understanding of the thermo-mechanical behaviour of an energy pile group under nonuniform heating conditions in which some of the energy piles in the group were not thermally active.

Table 3 Model test conditions used in this study

Test	Pile type	Load case	Thermal type	Thermal types map
Test 1	SP1	Ultimate load	Nonthermal	
Test 2	SP2	Working load (1.23 kN)	Thermal	
Test 3	3×3	Ultimate load	Nonthermal	
Test 4	3×3	Working load (11 kN)	All piles thermal	
Test 5	3×3	Working load (11 kN)	2×3 piles thermal	

● is the thermal pile; ○ is the nonthermal pile

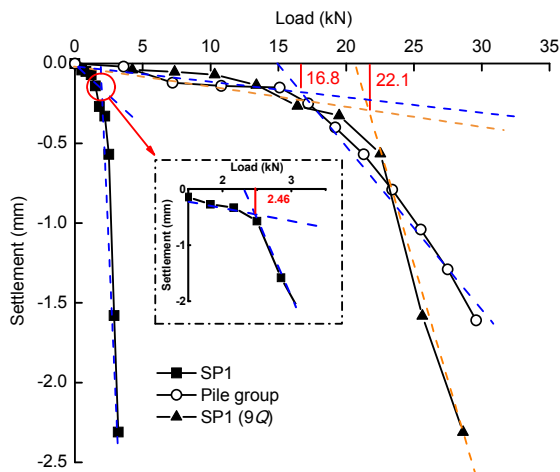


Fig. 6 Curve of load versus displacement of SP1 and pile group

5 Heat exchange behavior

As stated above, for testing the thermo-mechanical response of the single energy pile (SP2), water was circulated through its U-tube and the inlet temperature of the water followed the temperature

pattern in Fig. 5. Therefore, the shaft temperature of the pile changed with time to reflect the effect of the inlet controlled-temperature circulation process. The average shaft temperature of SP2 during the circulation process is shown Fig. 8. The results show that the change in the average temperature of the pile shaft was less than the change in the inlet temperature. This behaviour could be attributed to the expected reduction in the temperature of the circulating fluid as the depth increased due to heat exchange with the surrounding soil.

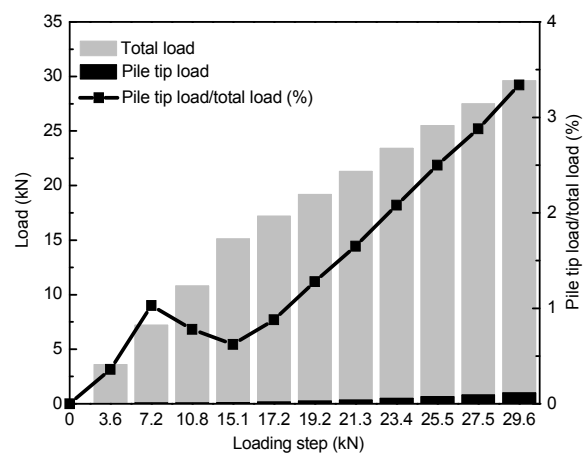


Fig. 7 Pile tip load and pile top load (total load) with the ratio between them of the pile group

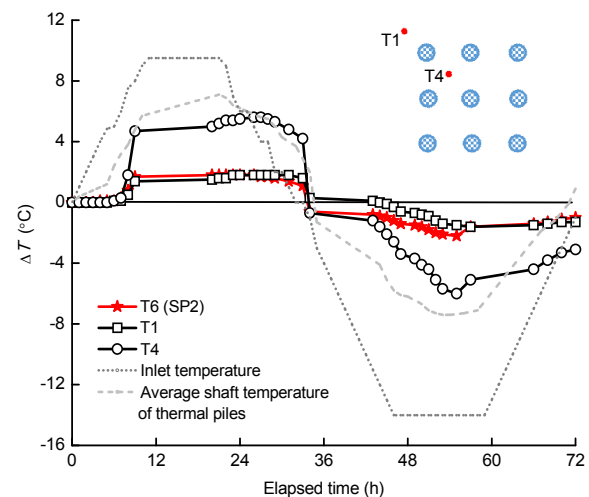


Fig. 8 Soil temperature of pile group (Test 4) and single pile (Test 2)

The change in soil temperature due to the heat exchange-circulation process at T6, which is located

at a radial distance of $2D$ from the center of SP2 and at a depth of 0.75 m from the soil surface (Fig. 1), is also plotted in Fig. 8. This result reflects the soil thermal resistance to dissipation of the heat exchanged at the surface of the energy pile. To assess the energy pile group effect on the soil, the thermal resistance response and the change in the soil temperature at point T1, which was located at a radial distance of $2D$ from the corner pile of the pile group and at a depth of 0.75 m from the soil surface, is also plotted in Fig. 8 for Test 4. The results in Fig. 8 reveal an approximately equal change in temperature at a radial distance of $2D$ from the single energy pile or from the corner of the energy pile group. The change in temperature at T4 shows that the soil within the energy pile group had a temperature similar to the average temperature of the shaft of the thermal pile (Fig. 8). This result suggests that for heat exchange purposes the energy pile group system could be simplified and represented as a block heat exchanger unit in which the cross-sectional area of the block includes the energy piles in the group and the soil between them, and its depth is equal to the length of the piles.

6 Thermally induced displacement of the single floating energy pile

The pile top and tip displacement of SP2 during the heat exchange operation (Test 2) is plotted in Fig. 9. For comparison, the thermal displacement at the top and tip of the pile under free thermal expansion conditions is also shown in Fig. 9. A positive displacement means the pile top or tip moves up whereas a negative displacement means the pile top or tip moves down. The results in Fig. 9 indicate that during the first heating phase the pile top displacement matched the free thermal expansion condition. This behaviour could be attributed to the low stress constraint condition on the pile because the pile axial load and the lateral confining pressure on the pile shaft were very small. However, during the subsequent cooling phase, the pile top moved down more than expected under the free condition. The difference between the observed pile top displacement and the free condition displacement results indicates that soil-pile slippage had occurred during the cooling phase. Soil-pile slippage is expected during the

cooling process as the pile and the surrounding soil contract as their temperature drops below the initial temperature (19 °C). The cooling-induced change in the contraction volume reduced the lateral confining pressure on the pile shaft. Consequently, the pile skin (shaft) friction resistance decreased and soil-pile slippage could occur.

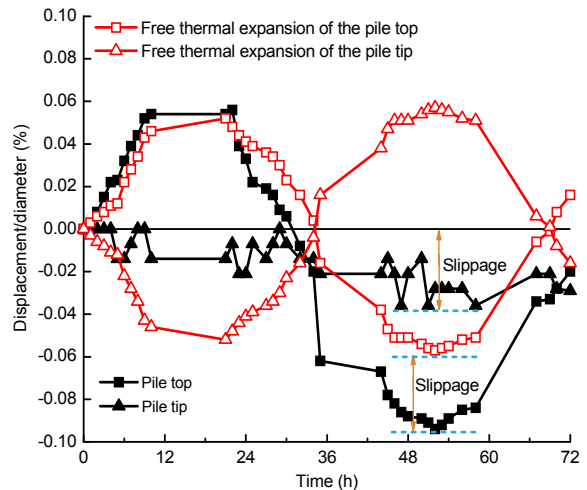


Fig. 9 Displacements of the pile top and pile tip of SP2

The results in Fig. 9 show that the pile tip moved down during the first heating phase. However, the magnitude of the downward movement was less than expected under the free condition. This behaviour is different from that of the pile top which almost followed expectation under the free condition. The difference between the displacement behaviour of the pile top and tip could be attributed to the change in the soil lateral confining pressure which increases with depth. The pile skin friction resistance increases as the soil lateral confining pressure increases, and therefore the lower part of the pile was expected to have a higher pile skin friction resistance than the top part. Therefore, the lower part of the pile was subjected to higher restrain boundary condition than the upper part of the pile, and less displacement is observed at the pile tip than at the pile top. Upon subjecting the pile to the subsequent cooling phase, the pile tip moved slightly downward instead of upward. We believe that the pile tip did move up under cooling. However, the observed downward movement was due mainly to the expected soil-pile slippage under the cooling condition.

7 Thermally induced displacement of the floating energy pile group

Fig. 10 shows the thermally induced displacements of the pile group cap at its two corners (GP1 & GP2), and the pile tips at three different time-temperature points, namely, Ta (end of first heating), Tb (end of cooling), and Tc (end of heating) (Fig. 4). The left side of Fig. 10 presents the results of the pile cap (top) whereas the right side shows the results of some of the pile tips in the group. For comparison, the thermal displacement of the single energy pile (SP2, Test 2) and the displacements under the free thermal condition are also shown in Fig. 10.

Fig. 10a includes the results of Test 4 in which all the piles in the group were thermally active (thermal pile). The results indicate that at Ta the pile cap moved up uniformly and with a magnitude similar to that of the upward movement of the single pile and the free displacement condition. However, upon cooling to Tb, the downward movement of the pile group cap was larger than that of the single pile and the free displacement condition. As mentioned earlier, the downward movement during the cooling process could be attributed to cooling-induced soil-pile slippage. As the lateral confining pressure for a pile in a group is less than that for a single pile due to the pile interaction effect (Poulos and Mattes, 1985), the cooling contraction effect on the pile skin friction resistance will be more significant in the case of a pile group than for a single pile. Consequently, more slippage is expected for the pile group case.

Upon heating back to Tc, the magnitude of upward movement U of the cap of the pile group, the top of the single pile, and the free thermal expansion condition were similar (Fig. 10a, left side). This behaviour indicates that the upward movement U is the thermal elastic pile top displacement part.

For the pile tips (Fig. 10a, right side), it is noticeable that the inner pile (P5) in the group had a thermal displacement behaviour different from that of P1 and P2. Moreover, the magnitude of the thermal displacements at the tip of P5, under Ta and Tb temperature conditions, was similar to the magnitude of displacements under free thermal expansion condition. As P5 was surrounded by piles in all directions, its pile interaction condition was different from that of the edge and the corner piles (Poulos and Mattes,

1985). Therefore, the lateral confining pressure of P5 was expected to be lower than that of the other piles in the group. Because the restraint level on P5 was lower, its tip had more freedom to move up or down as the temperature changed (Fig. 10a, right side).

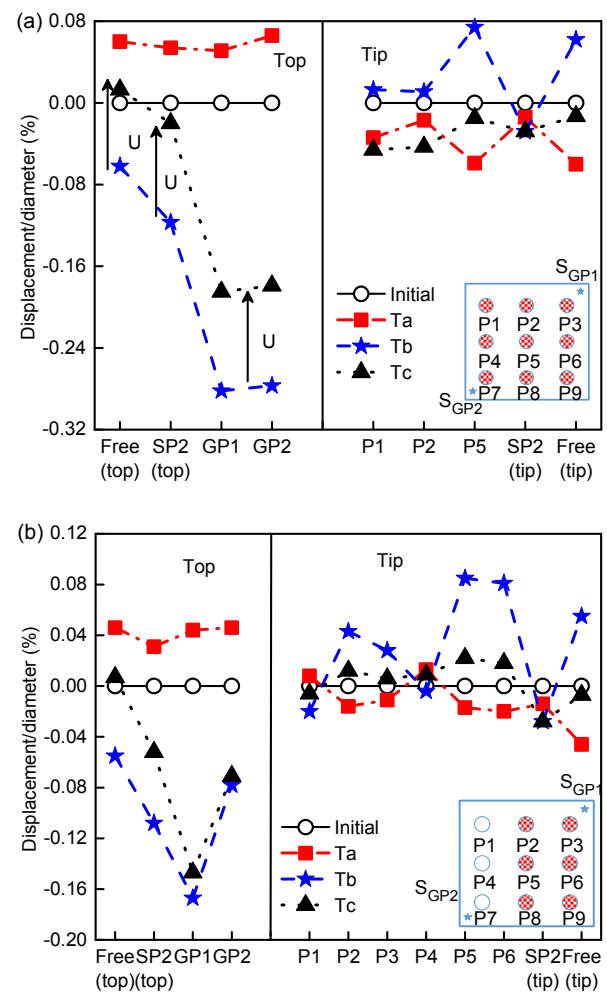


Fig. 10 Displacements of the pile group cap and the pile tips under uneven thermal: (a) Test 4; (b) Test 5

The results of Test 5 in which only six piles were thermally active (thermal pile) are shown in Fig. 10b. Similar to the results of Test 4 for the top cap of the pile group, as the temperature increased up to Ta, the top cap of the pile group moved upwards with a magnitude similar to that of the single pile case and the free thermal displacement condition. No tilt was observed in the cap of the group pile at Ta, although P1, P4, and P7 were nonthermal piles. This behaviour could be attributed to the high level of

rigidity of the pile cap and the low lateral confining pressure on the nonthermal piles. Therefore, the pull-out resistance of the nonthermal piles could be smaller than the thermally induced pull-out force of the thermal piles in the group. This explanation is supported by the tip displacement of the nonthermal pile P1 at Ta, which showed upward movement (Fig. 10b, right side).

Under the Tb condition, the skin friction resistance of thermal piles (P2, P3, P5, P6, P8, P9) would drop due to the cooling-induced contraction process. However, the skin friction resistance of nonthermal piles (P1, P4, P7) would be only slightly affected by the cooling process. Therefore, more soil-pile slippage was expected on the thermal pile side (GP1) (Fig. 10b, left side). Tilt occurred in the cap, as more downward movement was observed at GP1 than at GP2.

On the sides of the pile tip, the inner thermal piles (P5, P6) showed a higher displacement response than the other piles under the Tb case. It is not clear how this behaviour could be explained. However, we suggest that the observed tilt of the pile group cap at Tb (Fig. 10b, right side) could disturb the spring-load cell setup used to measure the tip pile displacement. Consequently, less accurate tip displacement readings might be obtained under tilting conditions.

8 Axial stresses in the pile group

According to Bourne-Webb et al. (2012) and Amatya et al. (2012), under the heating condition the maximum thermally induced axial stress of a single floating energy pile should be at the mid-length of the pile. At Ta, the results of Tests 4 and 5 agree with this postulation (Fig. 11). However, the results in Fig. 11 show that the thermally induced axial stress of the energy pile group, under heating condition (Ta), was always less than that of the single energy pile (SP2). This behavior can be explained in terms of the expected difference in the pile skin friction resistance between a single pile and a pile in a group, due to the pile group interaction effect (Poulos and Mattes, 1985). Pile skin friction is controlled by the lateral confining pressure. Due to the boundary condition effects, the lateral confining pressure of a single pile

is higher than that of a pile in a group. Consequently, the pile skin friction resistance of the single pile was higher than that of the pile group. As the thermally induced axial stress developed as a result of restraining the thermally induced axial displacement of the pile, and the pile skin friction is the restraining action that can restrict the axial thermal displacement, we deduce that as the pile skin friction increased the thermally induced axial strain increased. Therefore, the thermally induced axial stress of the single pile should be higher than that of a pile in a group (Fig. 11). This behaviour is also applicable to the case where some piles were nonthermal (Test 5) (Fig. 11b). Upon cooling (Tb), similar behaviour can be observed, but tension due to thermally induced axial stress will develop and reach a maximum at the mid-length of the pile (Fig. 11b).

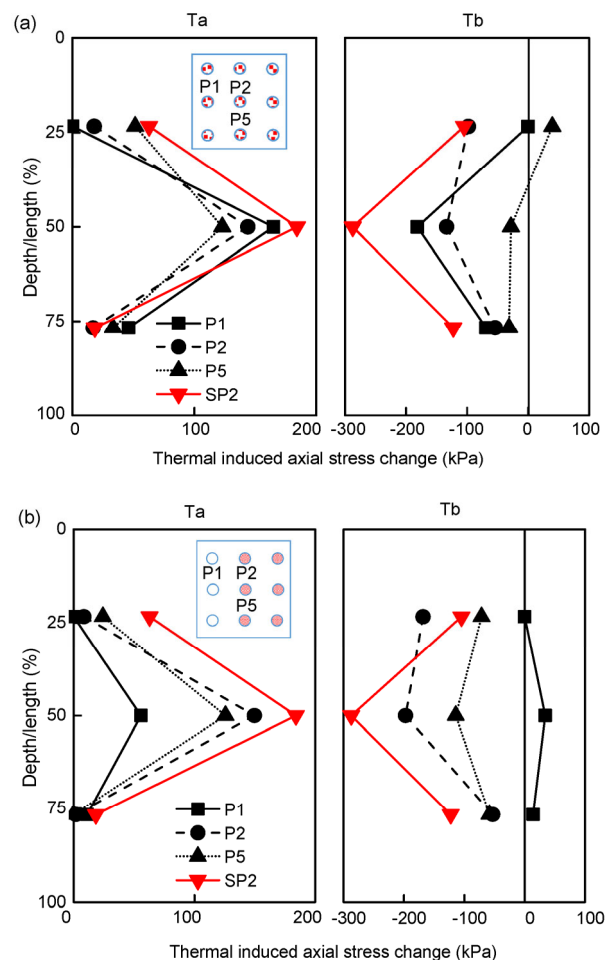


Fig. 11 Thermal induced axial stress change of floating pile group: (a) Test 4; (b) Test 5

9 Conclusions

In this study, small-scale model tests were conducted to understand the thermo-mechanical behaviour of a single energy floating pile and an energy floating pile group. The salient outcomes of this experimental study are as follows:

1. For long-term heat exchange analysis of an energy pile group, the results of this study suggest that the energy pile group could be represented as a block heat exchanger unit with a surface temperature equal to the average temperature of the energy pile surface. The heat exchanger block has a cross sectional area equal to the gross area of the pile group, and its length is equal to the pile length.

2. For the single energy floating pile, under the heating condition the pile top displacement was larger than the pile tip displacement as the restrained boundary condition (lateral confining pressure) was stronger in the lower half of the pile.

3. Under the cooling condition, the single floating pile showed a downward soil-pile slippage due to a cooling-induced volume contraction effect that reduced the lateral confining pressure on the pile and consequently reduced the pile skin friction resistance.

4. The thermal displacement of an energy floating pile group cap under the heating condition is a function of the restrained boundary condition of the top half of the pile group. As the small-scale tests conducted in this study had low confining pressure on the top half of the pile, the thermal displacement of the cap of the pile group was equal to the value of the free thermal condition.

5. Under the cooling condition, the pile-slippage magnitude of pile group was larger than that of the single pile, as the pile group interaction effect reduced the pile skin friction resistance.

6. The pile tip thermal displacement of the inner pile in the group showed more downward movement under the cooling condition since this pile had a higher pile interaction effect.

7. For the case where not all the piles in the group were thermally active, nonuniform displacement could occur. However, under the heating condition, this behaviour is a function of the pull-out resistance of the nonthermal pile, whereas under the cooling condition, it is controlled by the reduction in

the skin friction of the thermal pile due to the cooling-induced volume contraction behaviour.

8. The thermally induced axial pile stress change is a function of the restrained boundary condition of the pile, which is determined mainly by the lateral confining pressure on the floating pile. Therefore, as pile interaction could reduce the restrained condition of the pile group, the thermally induced axial stress was larger for the single pile than for a pile in a group.

References

- Amatya BL, Soga K, Bourne-Webb PJ, et al., 2012. Thermo-mechanical behaviour of energy piles. *Géotechnique*, 62(6):503-519.
<https://doi.org/10.1680/geot.10.P.116>
- Bourne-Webb PJ, Amatya B, Soga K, et al., 2009. Energy pile test at Lambeth College, London: geotechnical and thermodynamic aspects of pile response to heat cycles. *Géotechnique*, 59(3):237-248.
<https://doi.org/10.1680/geot.2009.59.3.237>
- Bourne-Webb PJ, Amatya B, Soga K, 2012. A framework for understanding energy pile behaviour. *Proceedings of the Institution of Civil Engineers-Geotechnical Engineering*, 166(2):170-177.
<https://doi.org/10.1680/geng.10.00098>
- Dave TN, Dasaka SM, 2012. Assessment of portable traveling pluviator to prepare reconstituted sand specimens. *Geomechanics and Engineering*, 4(2):79-90.
<https://doi.org/10.12989/gae.2012.4.2.079>
- Di Donna A, Laloui L, 2015. Numerical analysis of the geotechnical behaviour of energy piles. *International Journal for Numerical and Analytical Methods in Geomechanics*, 39(8):861-888.
<https://doi.org/10.1002/nag.2341>
- Goode III JC, McCartney JS, 2015. Centrifuge modeling of end-restraint effects in energy foundations. *Journal of Geotechnical and Geoenvironmental Engineering*, 141(8):1-13.
[https://doi.org/10.1061/\(ASCE\)GT.1943-5606.0001333](https://doi.org/10.1061/(ASCE)GT.1943-5606.0001333)
- Hariprasad C, Rajashekhar M, Umashankar B, 2016. Preparation of uniform sand specimens using stationary pluviation and vibratory methods. *Geotechnical and Geological Engineering*, 34(6):1909-1922.
<https://doi.org/10.1007/s10706-016-0064-0>
- Jeong S, Lim H, Lee JK, et al., 2014. Thermally induced mechanical response of energy piles in axially loaded pile groups. *Applied Thermal Engineering*, 71(1):608-615.
<https://doi.org/10.1016/j.applthermaleng.2014.07.007>
- Kalantidou A, Tang AM, Pereira JM, et al., 2012. Preliminary study on the mechanical behaviour of heat exchanger pile in physical model. *Géotechnique*, 62(11):1047-1051.
<https://doi.org/10.1680/geot.11.T.013>

- Kraft Jr LM, 1991. Performance of axially loaded pipe piles in sand. *Journal of Geotechnical Engineering*, 117(2):272-296.
[https://doi.org/10.1061/\(asce\)0733-9410\(1991\)117:2\(272\)](https://doi.org/10.1061/(asce)0733-9410(1991)117:2(272))
- Laloui L, Nuth M, Vulliet L, 2006. Experimental and numerical investigations of the behaviour of a heat exchanger pile. *International Journal for Numerical and Analytical Methods in Geomechanics*, 30(8):763-781.
<https://doi.org/10.1002/nag.499>
- Li M, Lai ACK, 2015. Review of analytical models for heat transfer by vertical ground heat exchangers (GHEs): a perspective of time and space scales. *Applied Energy*, 151: 178-191.
<https://doi.org/10.1016/j.apenergy.2015.04.070>
- Liu XC, Xu WJ, Zhan LT, et al., 2016. Laboratory and numerical study on an enhanced evaporation process in a loess soil column subjected to heating. *Journal of Zhejiang University-SCIENCE A (Applied Physics & Engineering)*, 17(7):553-564.
<https://doi.org/10.1631/jzus.A1600246>
- Lo Presti DCF, Berardi R, Pedroni S, et al., 1993. A new traveling sand pluviator to reconstitute specimens of well-graded silty sands. *Geotechnical Testing Journal*, 16(1):18-26.
<https://doi.org/10.1520/GTJ10263J>
- McCartney JS, Rosenberg JE, 2011. Impact of heat exchange on side shear in thermo-active foundations. *Geo-Frontiers 2011: Advances in Geotechnical Engineering*, p.488-498.
[https://doi.org/10.1061/41165\(397\)51](https://doi.org/10.1061/41165(397)51)
- Mimouni T, Laloui L, 2015. Behaviour of a group of energy piles. *Canadian Geotechnical Journal*, 52(12):1913-1929.
<https://doi.org/10.1139/cgj-2014-0403>
- Murphy KD, McCartney JS, Henry KS, 2015. Evaluation of thermo-mechanical and thermal behavior of full-scale energy foundations. *Acta Geotechnica*, 10(2):179-195.
<https://doi.org/10.1007/s11440-013-0298-4>
- Ng CWW, Shi C, Gunawan A, et al., 2014. Centrifuge modelling of energy piles subjected to heating and cooling cycles in clay. *Géotechnique Letters*, 4(4):310-316.
<https://doi.org/10.1680/geolett.14.00063>
- Poulos HG, Mattes NS, 1985. Settlement and load distribution analysis of pile groups. In: *Golden Jubilee of the International Society for Soil Mechanics and Foundation Engineering: Commemorative Volume*. Institution of Engineers, Barton, Australia, p.155-165.
- Rotta Loria AF, Laloui L, 2017a. Thermally induced group effects among energy piles. *Géotechnique*, 67(5):374-393.
<https://doi.org/10.1680/jgeot.16.P.039>
- Rotta Loria AF, Laloui L, 2017b. The equivalent pier method for energy pile groups. *Géotechnique*, 67(8):691-702.
<https://doi.org/10.1680/jgeot.16.P.139>
- Rotta Loria AF, Laloui L, 2017c. Displacement interaction among energy piles bearing on stiff soil strata. *Computers and Geotechnics*, 90:144-154.
<https://doi.org/10.1016/j.compgeo.2017.06.008>
- Saggu R, Chakraborty T, 2016. Thermomechanical response of geothermal energy pile groups in sand. *International Journal of Geomechanics*, 16(4):1-13.
[https://doi.org/10.1061/\(asce\)gm.1943-5622.0000567](https://doi.org/10.1061/(asce)gm.1943-5622.0000567)
- Salciarini D, Ronchi F, Cattoni E, et al., 2013. Thermomechanical effects induced by energy piles operation in a small piled raft. *International Journal of Geomechanics*, 15(2):04014042.
[https://doi.org/10.1061/\(asce\)gm.1943-5622.0000375](https://doi.org/10.1061/(asce)gm.1943-5622.0000375)
- Salciarini D, Ronchi F, Tamagnini C, 2017. Thermo-hydro-mechanical response of a large piled raft equipped with energy piles: a parametric study. *Acta Geotechnica*, 12(4): 703-728.
<https://doi.org/10.1007/s11440-017-0551-3>
- Salgado R, Mitchell JK, Jamiolkowski M, 1998. Calibration chamber size effects on penetration resistance in sand. *Journal of Geotechnical and Geoenvironmental Engineering*, 124(9):878-888.
[https://doi.org/10.1061/\(asce\)1090-0241\(1998\)124:9\(878\)](https://doi.org/10.1061/(asce)1090-0241(1998)124:9(878))
- Stewart MA, McCartney JS, 2014. Centrifuge modeling of soil-structure interaction in energy foundations. *Journal of Geotechnical and Geoenvironmental Engineering*, 140(4):04013044.
[https://doi.org/10.1061/\(ASCE\)GT.1943-5606.0001061](https://doi.org/10.1061/(ASCE)GT.1943-5606.0001061)
- Wang B, Bouazza A, Singh RM, et al., 2014. Posttemperature effects on shaft capacity of a full-scale geothermal energy pile. *Journal of Geotechnical and Geoenvironmental Engineering*, 141(4):04014125.
[https://doi.org/10.1061/\(asce\)gt.1943-5606.0001266](https://doi.org/10.1061/(asce)gt.1943-5606.0001266)
- Wang CL, Liu HL, Kong GQ, et al., 2016. Model tests of energy piles with and without a vertical load. *Environmental Geotechnics*, 3(4):203-213.
<https://doi.org/10.1680/jenge.15.00020>
- Wang CL, Liu HL, Kong GQ, et al., 2017. Different types of energy piles with heating-cooling cycles. *Proceedings of the Institution of Civil Engineers-Geotechnical Engineering*, 170(3):220-231.
<https://doi.org/10.1680/jgeen.16.00061>
- Wang TF, Liu JK, Zhao HG, et al., 2016. Experimental study on the anti-jacking-up performance of a screw pile for photovoltaic stents in a seasonal frozen region. *Journal of Zhejiang University-SCIENCE A (Applied Physics & Engineering)*, 17(7):512-524.
<https://doi.org/10.1631/jzus.A1600407>
- You S, Cheng XH, Guo HX, et al., 2014. In-situ experimental study of heat exchange capacity of CFG pile geothermal exchangers. *Energy and Buildings*, 79:23-31.
<https://doi.org/10.1016/j.enbuild.2014.04.021>
- You S, Cheng XH, Guo HX, et al., 2016. Experimental study on structural response of CFG energy piles. *Applied Thermal Engineering*, 96:640-651.
<https://doi.org/10.1016/j.applthermaleng.2015.11.127>

中文概要

题目: 砂土地基中摩擦型能量桩群桩热力学特性研究

目的: 能量桩在工作状态下的热力学响应十分复杂, 同时受到桩顶荷载、桩侧摩擦以及温度等多重因素的影响。当群桩中出现部分能量桩不工作时, 将造成上部结构的额外应力与变形。因此, 本文重点探讨摩擦型能量桩群桩中部分能量桩在加热制冷作用下的热力学响应, 并与单桩的热力学效应进行对比分析。

创新点: 1. 通过建立摩擦型能量桩群桩模型试验, 探讨桩侧摩擦对能量桩群桩的影响规律; 2. 利用能量桩群桩与单桩对比, 揭示能量桩群桩与单桩热力响应特性的区别; 3. 揭示部分能量桩加热制冷作用对能量桩群桩的影响机理。

方法: 1. 建立摩擦型能量桩群桩及单桩的模型试验; 2. 将能量桩群桩与单桩进行对比, 研究能量桩群桩与单桩热力响应特性的区别; 3. 进行能量桩群桩部分加热制冷试验。

结论: 1. 对于长期工作的能量群桩, 可以将其视为一个长宽高与整个群桩相同的热交换体, 其表面温度

与群桩的平均表面温度一致。2. 能量桩单桩在加热过程中, 由于桩底受到的限制较大, 所以桩顶位移大于桩底位移。3. 能量桩单桩在制冷过程中, 由于土体及桩体收缩, 会出现明显的下沉。4. 能量桩群桩桩帽在加热过程中, 桩帽的位移与群桩的上半部分长度相关; 在本文的试验中, 由于群桩上半部分受土的限制较小, 因此其位移与桩自由膨胀的位移一样。5. 能量桩群桩在制冷期间, 群桩的下沉量级要比单桩的大。6. 在制冷过程中, 能量桩群桩在群桩效应作用下, 内部桩的桩底热位移较大。7. 能量桩群桩在部分加热的情况下, 会出现不均匀沉降, 且在加热期间, 沉降主要受到不工作桩的牵制影响; 而在制冷期间, 沉降主要受工作桩的下沉影响。8. 摩擦型能量桩的热引起的桩身轴力是与桩侧的土压力大小相关的; 由于群桩在群桩效应作用下, 桩侧土压力要小于单桩, 因此群桩的热引起的桩身轴力要大于单桩。

关键词: 能量桩; 纯摩擦型桩; 群桩; 不均匀加热; 不均匀沉降